A Spiking Neuron and Population Model based on the Growth Transform Dynamical System

Ahana Gangopadhyay[1], Darshit Mehta[2], and Shantanu Chakrabartty[1]

[1]Department of Electrical and Systems Engineering, Washington University in St. Louis
[2]Department of Biomedical Engineering, Washington University in St. Louis

Abstract

This paper introduces a new spiking neuron and population model based on a Growth Transform dynamical system. The model allows integration and control of two different types of dynamics: (a) sub-threshold dynamics that determines the fixed-point solution of an underlying network objective or energy functional; and (b) a modulating super-threshold dynamics that controls the trajectory followed by the neurons to converge to the fixed-point solution. As a result, a recurrent and coupled network of the proposed growth transform neurons produces stable and interpretable population dynamics irrespective of the network size and interconnect complexity. In this paper, we present several variants of the neuron model that have been configured to produce different types of population encoding. One such variant described in this paper is a network that adapts itself according to the global dynamics to encode the steady-state solution with a reduced number of spikes. A publicly available software tool implementing the proposed model can be used by researchers to explore or customize new neuron-level and network-level dynamics.

Keywords— Spiking neuron model, Growth transform dynamical system, energy minimization, neural dynamics, population model.

1 Introduction

Physical processes occurring in nature have a universal tendency to move towards a minimum-energy state, defined by a configuration of the process variables, that is a function of the inputs and the state of the process. In neuroscience as well, a prevailing hypothesis states that a biological network can be modeled as an unified dynamical system where the spiking activity of populations of neurons results from an emergent behavior of an underlying optimization process. For instance, this underlying process could optimize some network-level metric (for example, system energy), while satisfying physical constraints imposed by evolution and biology. This hypothesis has resulted in several optimization-based approaches which include coupled-oscillator models [1], reservoir-based approaches and recurrent networks [2, 3] and other statistical physics based approaches [4, 5, 6, 7], to design neural dynamical systems that exhibit a rich set of trajectories. Energy-functions of spike-based network states have also been considered, where individual neuron states are assumed to be binary in nature (spiking or not spiking) [8] or replaced by their average firing rates [9]. Energy has also been modeled as an external resource to constrain and control neural activity [10]. However, there is a lack of an unified model in literature that treats the spike generation process as the direct derivative of optimizing an energy functional of continuous-valued neural variables (e.g. membrane potential) that can be used not only to mimic known neural dynamics observed in neurobiology, but also enable spike-based encoding and learning within an energy-based framework similar to traditional machine learning models [11].

Algorithm 1: Summary of the proposed Growth Transform based spiking neuron model.

For a network of N neurons with state variables $\mathbf{v} = \{v_i\} \in \mathcal{R}^N$, where the synaptic weight matrix is denoted by $\mathbf{Q} = \{Q_{ij}\} \in \mathcal{R}^N \times \mathcal{R}^N$ and the external stimulus vector is denoted by $\mathbf{b} = \{b_i\} \in \mathcal{R}^N$, the spike response of the i-th neuron at time t is given by

$$s_i(t) = v_i(t) + h\mathcal{I}[v_i(t) > 0]. \tag{1}$$

Here, h determines the magnitude of each spike, and $v_i(t)$ is governed by the following first-order dynamical system:

$$\frac{1}{f_i(t)}\frac{dv_i(t)}{dt} + v_i(t) = \frac{-g_i(t) + \lambda v_i(t)}{-v_i(t)g_i(t) + \lambda}, \tag{2}$$

where

$g_i(t) = \sum_{j=1}^{N} Q_{ij}v_j(t) - b_i(t) + \Psi(v_i(t))$;

$\Psi(v_i(t)) = \left\{ \begin{array}{ccc} C & ; & v_i(t) > 0 \\ 0 & ; & v_i(t) \leq 0 \end{array} \right\}$;

λ is a fixed hyper-parameter such that $\lambda > |g_i(t)| \ \forall i, t$;

$0 \leq f_i(t) \leq 1$ is a modulation function that controls the trajectory.

In [12], we proposed a model of a Growth Transform (GT) neuron whose dynamical and spiking responses were shown to be strongly coupled with the network objective function. It was shown that while each individual neuron traverses a trajectory in the dual optimization space, the overall network traverses a trajectory in an equivalent primal optimization space. As a result, the network of growth transform neurons was shown to solve binary classification tasks, while producing stable, unique but interpretable neural dynamics like noise-shaping, spiking and bursting which encoded margin information. In this paper, we generalize this framework to describe the model of a spiking neuron whose responses are similarly derived from minimizing a network objective function which is a measure of the extrinsic energy needed by the network to operate, and which is flexible enough to incorporate neurodynamics that have been experimentally observed [13]. We first introduce a dynamical system of first-order differential equations based on Growth Transforms that minimizes a Lipschitz continuous objective function when the optimization variables are bounded, and present a proof of convergence. We then introduce a form of the objective function for a non-spiking variant of a neuron model using this dynamical system based on a simple model for network energy, and extend it to a spiking variant that asymptotically minimizes the network energy. The key advantage of this model is that it allows integration and control of two different dynamics: (a) a dominant dynamics that determines the fixed-point solution of the network objective or energy functional; and (b) a modulating dynamics that controls the trajectory followed by the neurons to converge to the fixed-point solution. The latter can be tuned in a multitude of ways to program the neuron to exhibit different neural dynamics and response characteristics without affecting the underlying energy minimization process. The framework can be easily extended to implement a network of coupled neurons that can exhibit memory, global adaptation, and other interesting population dynamics under different initial conditions and based on different network states. For the ease of exposition, a summary of the proposed spiking neuron model is described in Table 1, and the rest of the paper presents the derivation of this model, along with some examples of different dynamics that could be generated using this model. This paper is also accompanied by a publicly available software implementing the proposed model [14] using MATLAB ©. Users

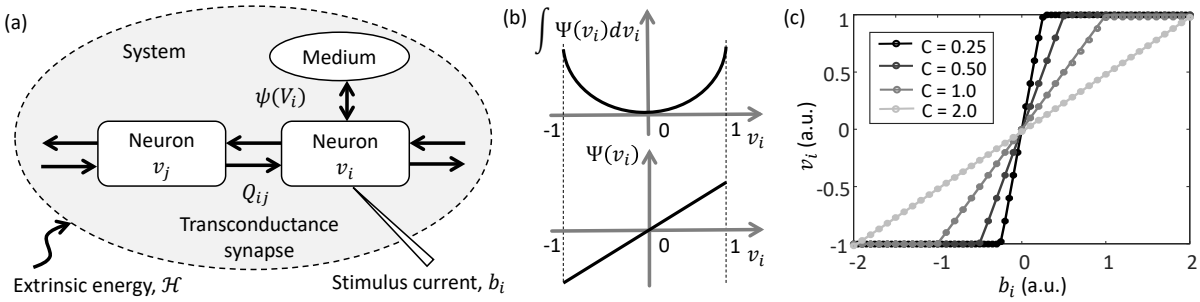

Figure 1: (a) A compartment model used for approximating the power influx and power dissipated/injected due to the process of spike generation, spike transmission and stimulation; (b) A quadratic form of the function $\int \Psi(v_i)dv_i$ in (16) and its corresponding derivative $\Psi(.)$; (c) Input-output characteristics of the non-spiking neuron model for different values of C.

can experiment with different inputs and network parameters to explore and create other unique dynamics.

The paper is organized as follows. Section 2 presents the dynamical system based on Growth Transforms, along with an outline of the proof of its convergence. Section 3 presents the non-spiking Growth Transform neuron model based on this dynamical system, and Section 4 extends it to the model of a spiking neuron. Section 5 illustrates how the proposed model can be tuned to exhibit different neural dynamics at the level of a single neuron, as well as when several neurons are connected together through synaptic weights to form a network. Finally in Section 6, we conclude this paper with a discussion about the scope of future research in this area.

2 Growth transform dynamical system

For the sake of accessibility, we first present the dynamical system model using scalar functions and scalar variables before extending it to the domain of vectors. Also, to simplify the mathematical notations, we will interchangeably use the continuous-time and and discrete-time representations of the state variable $v(t) \in \mathcal{R}$ as $v(t) \equiv v_n$, where $n \in \mathcal{N}$ denotes the discrete-time index. Similarly, $\frac{dv}{dt} \equiv \Delta v_n = v_{n+1} - v_n$.

Theorem. Let $\mathcal{H}(v_n) : \mathcal{R} \rightarrow \mathcal{R}$ be a Lipschitz-continuous function of v_n, with $\lambda > |\frac{\partial \mathcal{H}}{\partial v_n}|$ being a hyper-parameter. If $f_n \in [0, 1]$ denotes a time-varying function, then for $|v_0| \leq 1$, the dynamical system

$$\frac{1}{f_n}\Delta v_n + v_n = \frac{\frac{-\partial \mathcal{H}}{\partial v_n} + \lambda v_n}{-v_n \frac{\partial \mathcal{H}}{\partial v_n} + \lambda} \tag{3}$$

satisfies the following criteria for all time-indices n:

$$(a)\ |v_n| \leq 1 \tag{4}$$

$$(b)\ \mathcal{H}(v_n) \leq \mathcal{H}(v_{n-1}) \tag{5}$$

$$(c) \lim_{n\rightarrow\infty}\ (v_n^2 - 1)\frac{\partial \mathcal{H}}{\partial v_n} \rightarrow 0. \tag{6}$$

Proof. We can decompose the scalar variable v_n as $v_n = v_n^+ - v_n^-$, where $v_n^+, v_n^- \geq 0$. The following additional constraint

$$v_n^+ + v_n^- = 1 \tag{7}$$

imposed on the variables v_n^+ and v_n^- would then always ensure that (a) is satisfied. Then we can write

$$\arg\min_{v}\ \mathcal{H}(v) \equiv \arg\min_{v^+, v^-}\ \mathcal{H}(v^+ - v^-). \tag{8}$$

We can solve the equivalent optimization problem under the linear constraint specified by (7) using an iterative multiplicative update called Growth Transforms - a fixed point algorithm for optimizing any Lipschitz continuous objective function under similar equality constraints [15, 16].

The homotopically increasing property of Growth Transforms [17] leads to the following discrete-time update equations for the new optimization variables for minimizing $\mathcal{H}$

$$v_{n+1}^{+} = (1-f_n)v_n^{+} + f_n \frac{v_n^{+}}{\mu_n}(-\frac{\partial \mathcal{H}}{\partial v_n^{+}} + \lambda) \tag{9}$$

$$v_{n+1}^{-} = (1-f_n)v_n^{-} + f_n \frac{v_n^{-}}{\mu_n}(-\frac{\partial \mathcal{H}}{\partial v_n^{-}} + \lambda), \tag{10}$$

where $0 \leq f_n \leq 1$, and

$$\mu_n = v_n^{+}(-\frac{\partial \mathcal{H}}{\partial v_n^{+}} + \lambda) + v_n^{-}(-\frac{\partial \mathcal{H}}{\partial v_n^{-}} + \lambda) \tag{11}$$

is a normalization factor that ensures $v_{n+1}^{+} + v_{n+1}^{-} = 1$. From (9) and (10), using $v_n = v_n^{+} - v_n^{-}$ and (7), we can easily show

$$v_{n+1} = (1-f_n)v_n + f_n \frac{-\frac{\partial \mathcal{H}}{\partial v_n} + \lambda v_n}{-v_n \frac{\partial \mathcal{H}}{\partial v_n} + \lambda}, \tag{12}$$

where we have used the relation $\frac{\partial \mathcal{H}}{\partial v} = \frac{\partial \mathcal{H}}{\partial v^{+}} = -\frac{\partial \mathcal{H}}{\partial v^{-}}$. Rearranging the terms in (12), we can write

$$\begin{aligned} \frac{1}{f_n}\left[v_{n+1} - v_n\right] + v_n &= \frac{-\frac{\partial \mathcal{H}}{\partial v_n} + \lambda v_n}{-v_n \frac{\partial \mathcal{H}}{\partial v_n} + \lambda}, \text{ or} \\ \frac{1}{f_n}\Delta v_n + v_n &= \frac{-\frac{\partial \mathcal{H}}{\partial v_n} + \lambda v_n}{-v_n \frac{\partial \mathcal{H}}{\partial v_n} + \lambda}. \end{aligned} \tag{13}$$

This dynamical system model, derived from the Growth Transform updates outlined in (9) and (10), ensures that (b) holds, with equality being satisfied iff v_n is a critical point of $\mathcal{H}$.

In the limit when the network reaches a fixed point, using $\lim_{n\to\infty} v_{n+1} = v_n$, we have

$$v_n = \frac{-\frac{\partial \mathcal{H}}{\partial v_n} + \lambda v_n}{-v_n \frac{\partial \mathcal{H}}{\partial v_n} + \lambda}. \tag{14}$$

Rearranging the terms, we get (c). This guarantees that as long $|v_n| < 1$, the gradient $\frac{\partial \mathcal{H}}{\partial v_n}$ asymptotically goes to zero.

Extending this to a vector dynamical system where $\mathcal{H} : \mathcal{R}^N \to \mathcal{R}$ is a function of $\boldsymbol{v}_n = \{v_{1,n}, v_{2,n}, .., v_{N,n}\}$, we can write

$$\frac{1}{f_{i,n}}\Delta v_{i,n} + v_{i,n} = \frac{-\frac{\partial \mathcal{H}}{\partial v_{i,n}} + \lambda v_{i,n}}{-v_{i,n} \frac{\partial \mathcal{H}}{\partial v_{i,n}} + \lambda}, \quad i = 1, ..., N. \tag{15}$$

Here, λ is admissible iff $\lambda > |\frac{\partial \mathcal{H}}{\partial v_{i,n}}| \ \forall i, n$.

3 Compartmental Energy Minimization Model

Next we present a form of the objective function $\mathcal{H}$ that approximates the power dissipated in a neuronal network. We will use a simple compartment to designate a neuron i, as shown in Fig. 1, and the inter-cellular potential associated with neuron i will be denoted by v_i. Each neuron i

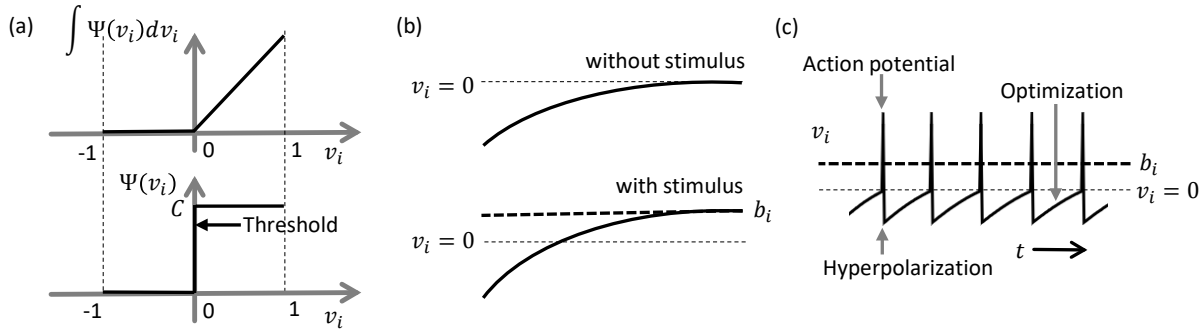

Figure 2: (a) The function $\int \Psi(v_i)dv_i$ and its derivative $\Psi(.)$ used in this paper for the spiking neuron model; (b) Time-evolution of the response v_i of a single neuron in the absence and presence of external stimulus without $\Psi(.)$; (c) Time-evolution of the response v_i of a single neuron in presence of external stimulus with $\Psi(.)$.

receives electrical input from neuron j through a synapse which is modeled as a conductance Q_{ij} [18]. As shown in Fig. 1, the neuron i also receives an electrical current stimuli b_i and exchanges voltage-dependent ionic-current with its medium, denoted by $\Psi(v_i)$. Thus, the total power influx or the energy influx over a fixed time-window, denoted by $\mathcal{H}$, for a network of N neurons can be written as

$$\mathcal{H} = \frac{1}{2}\sum_{i=1}^{N}\sum_{j=1}^{N} Q_{ij}v_jv_i - \sum_{i=1}^{N} b_iv_i + \sum_{i=1}^{N}\int \Psi(v_i)dv_i. \tag{16}$$

$\mathcal{H}$ in (16) comprises of three components: (a) Power dissipation due to synaptic interactions between neurons; (b) Power injected to or extracted from the system as a result of external stimulation; and (c) Power dissipated due to neural responses. Thus, $\mathcal{H}$ represents the extrinsic (or metabolic) power supplied to the network, and hence a quantity needed to be minimized based on evolutionary principles. To show the dynamics resulting from substituting (16) in the Growth Transform dynamical system in (15), we first consider $\Psi(.)$ such that its integral $\int \Psi(v_i)dv_i$ over $[-1, 1]$ is a smooth and convex function.

Rewriting (15) in terms of the objective function for the neuron model, we get

$$\frac{1}{f_{i,n}}\Delta v_{i,n} + v_{i,n} = g_i(v_n), \;\; i = 1, ..., N, \tag{17}$$

where

$$g_i(v_n) = \frac{-\sum_{j=1}^{N} Q_{ij}v_{j,n} + b_{i,n} - \Psi(v_{i,n}) + \lambda v_{i,n}}{-\sum_{j=1}^{N} Q_{ij}v_{j,n}v_{i,n} + b_{i,n}v_{i,n} - v_{i,n}\Psi(v_{i,n}) + \lambda}. \tag{18}$$

The steady-state, first-order potential $v_i = \lim_{n\to\infty} v_{i,n}$ is given by

$$(v_i^2 - 1)\frac{\partial \mathcal{H}}{\partial v} = 0 \tag{19}$$

which leads to the following response for the i-th neuron:

$$v_i = \begin{cases} \Psi^{-1}\left(-\sum_{j=1}^{N} Q_{ij}v_j + b_i\right) & ; \quad |v_i| < 1 \\ 1 & ; \quad v_i \geq 1 \\ -1 & ; \quad v_i \leq -1 \end{cases} \tag{20}$$

The nature and shape of $\int \Psi(v_i)dv_i$ determines the compressive response of the neuron given the pre-synaptic input and the input stimuli. For example, a quadratic form of $\int \Psi(v_i)dv_i$

shown in Fig. 1(b) and its corresponding derivative $\Psi(v_i) = Cv_i$ gives rise to an input-output characteristic shown in Fig. 1(c) for different values of the slope parameter C. Note that unlike conventional artificial neuron models, which uses an explicit compressive non-linearity like sigmoid or tanh, the growth-transform dynamical system generates a compressive response as a first-order condition of an underlying optimization problem. We show that this framework could also be extended to a spiking neuron model based on a gradient-discontinuous $\Psi(v_i)$.

4 Growth Transform Spiking neuron model

Neurons react to synaptic inputs and external stimuli and propagate signals to other neurons by producing a rapid change in their transmembrane current resulting in an action potential or a spike. In the compartmental model described in (16), the transmembrane current can be approximated by a non-smooth $\Psi(.)$. Fig. 2(a) shows a form of $\Psi(.)$ that has a gradient discontinuity at a threshold ($v_i = 0$) at which the neuron generates an action potential. Fig. 2(a) also shows the form of $\int \Psi(v_i)dv_i$ which models the power dissipation due to the spiking activity. Due to the gradient discontinuity, the growth-transform dynamical system described in (15) might not reach the critical point and some of the variables v_i, i.e. the ones that exceed the threshold for a given input and network configuration, will exhibit limit-cycle oscillations. However, if we assume that the limit-cycles are asymptotically stable where v_i can be treated as a random-variable with a stationary probability distribution, we can demonstrate the equivalence between the first-order spiking and non-spiking neuron model. We first define an expectation operator $\mathcal{E}(.)$ for a discrete-time signal x_n as

$$\mathcal{E}_n(x_n) = \lim_{K\to\infty} \frac{1}{K} \sum_{n=1}^{K} x_n, \tag{21}$$

and for a continuous-time signal $x(t)$ as

$$\mathcal{E}_t(x(t)) = \lim_{T\to\infty} \frac{1}{T} \int_{t=0}^{T} x(t)dt. \tag{22}$$

Minimizing $\mathcal{H}$ in (16) leads to the following stochastic first-order condition

$$\mathcal{E}_n \left[\frac{\partial \mathcal{H}}{\partial v_n} \right] \quad \rightarrow \quad 0, \text{ or} \tag{23}$$

$$\mathcal{E}_n \left[\Psi(v_{i,n}) \right] \quad \rightarrow \quad \mathcal{E}_n \left[-\sum_{j=1}^{N} Q_{ij} v_{j,n} + b_{i,n} \right], \tag{24}$$

The function $\Psi(.)$ used in this paper is given by

$$\Psi(v_{i,n}) = \begin{cases} C & ; \quad v_{i,n} > 0 \\ 0 & ; \quad v_{i,n} \leq 0 \end{cases} \tag{25}$$

where C is a parameter that determines the degree of hyperpolarization following a spike. To understand the process of spike-generation, we first show how v_i changes with and without the addition of $\Psi(.)$ in $\mathcal{H}$. Fig. 2(b) shows the response of a single neuron without $\Psi(.)$. Here, the response converges to the fixed point $v_i = 0$ in the absence of an external stimulus b_i. When a positive stimulus b_i is applied, the fixed-point shifts to a level that is a function of the magnitude of the stimulus. Once $\Psi(.)$ is introduced, as shown in Fig. 2(c), the potential v_i switches when $\Psi(v_i) > 0$ or only when $v_i > 0$. However, the dynamics of v_i remains unaffected for $v_i < 0$. During the brief period when $v_i > 0$, we assume that the neuron enters into a runaway state

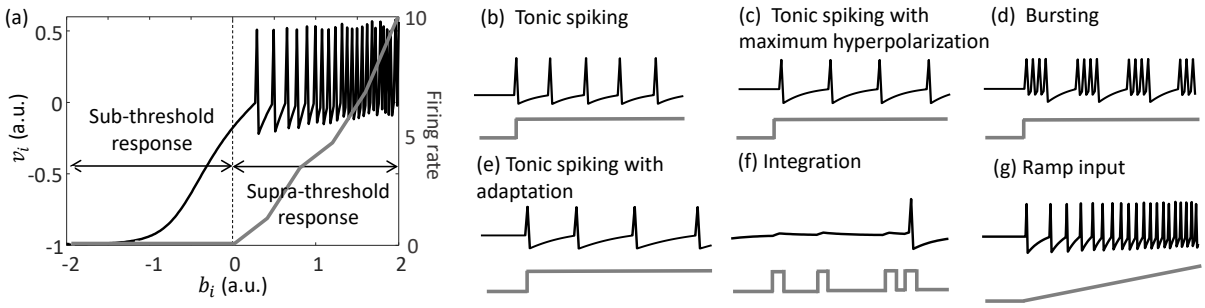

Figure 3: (a) Input-output characteristics of the spiking neuron model in terms of the membrane potential v_i and the firing rate over a time-window; (b)-(g) Simulations demonstrating different single-neuron responses obtained using the GT neuron model.

leading to a voltage spike. The composite spike signal $s_i(t)$ is then treated as a combination of the sub-threshold and supra-threshold responses and is given by

$$s_i(t) = v_i(t) + h\mathcal{I}[v_i(t) > 0], \tag{26}$$

where the constant $h > 0$ determines the magnitude of the spike. Note that in the current version, the proposed model does not explicitly model the runaway process that leads to the spike, unlike other neuron models [19, 20, 21].

Assuming that under asymptotic conditions, if v_i admits a stationary probability density function $p_v(v_{i,n})$, then

$$\begin{aligned}
\mathcal{E}_n[\Psi(v_{i,n})] &= \int_{-\infty}^{\infty} C\mathcal{I}[v_{i,n} > 0] p_v(v_{i,n}) dv_{i,n} \\
&= C \int_{0}^{\infty} p_v(v_{i,n}) dv_{i,n} \\
&\geq C \int_{0}^{\infty} v_{i,n} p_v(v_{i,n}) dv_{i,n} \\
&\geq C \int_{-\infty}^{\infty} v_{i,n} p_v(v_{i,n}) dv_{i,n} \\
&= C\mathcal{E}_n[v_{i,n}],
\end{aligned} \tag{27}$$

since $-1 \leq v_{i,n} \leq 1$. For $C \geq 1$, we can then rewrite (24) as

$$\begin{aligned}
\mathcal{E}_n[v_{i,n}] &\leq \mathcal{E}_n\left[-\sum_{j=1}^{N} Q_{ij} v_{j,n} + b_{i,n}\right] \\
&\rightarrow \Phi\left(-\sum_{j=1}^{N} Q_{ij} \mathcal{E}_n\left[v_{j,n}\right] + \mathcal{E}_n\left[b_{i,n}\right]\right),
\end{aligned} \tag{28}$$

where $\Phi(.)$ designates a compressive non-linearity. Thus, (28) can be viewed as a stochastic variant of the first-order conditions given by (20), that minimizes the objective function in (16) over the empirical time-averaged variables v_i and stimuli b_i. Note that for the form of $\int \Psi(.)$ and if the synaptic matrix $\mathbf{Q}$ is assumed to be positive-definite, the network function $\mathcal{H}$ is convex. Therefore, asymptotically the network exhibits limit-cycles about a single attractor or a fixed-point. A similar stochastic first-order framework was used in [22] to derive a dynamical system corresponding to $\Sigma\Delta$ modulation for tracking low-dimensional manifolds embedded in high-dimensional analog signal spaces. The operation of the neuron is governed by two sets of

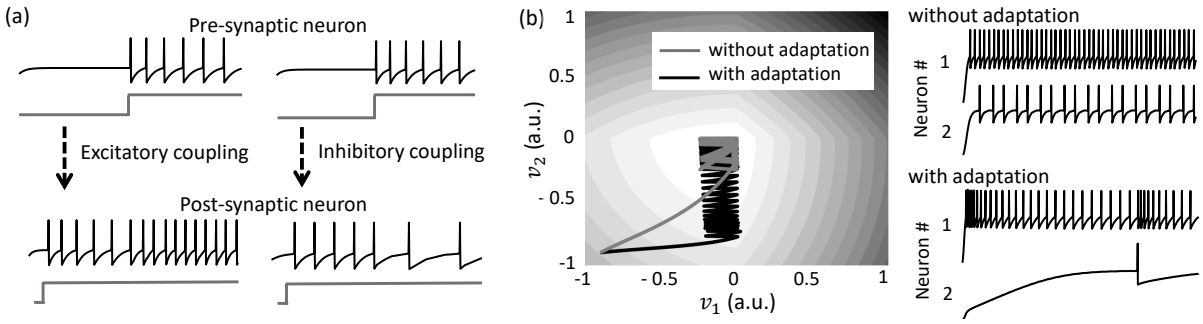

Figure 4: (a) Results from a 2-neuron network with excitatory and inhibitory couplings; (b) Energy optimization process under different conditions lead to different limit cycles within the same energy landscape.

dynamics: (a) minimization of the network energy functional $\mathcal{H}$; (b) modulation of the trajectory using the parameter $f_{i,n}$ which can be time-varying and individually tuned for each neuron. Fortunately, the evolution of $f_{i,n}$ can be made as complex as possible without affecting the asymptotic fixed-point solution of the optimization process. In the next section, we present a detailed overview of the neuron model and its parameters, and show how different forms of $f_{i,n}$ produce different sets of neuronal dynamics consistent with the dynamics that have been reported in neurobiology.

5 Growth Transform Neural Dynamics

Single neurons show a vast repertoire of response characteristics and dynamical properties that lend richness to their computational properties at the network level. Izhikevich in [13] provides an extensive review of different spiking neuron models and their ability to produce the different dynamics observed in biology. In this section, we show how we can reproduce a vast majority of such dynamics by changing the modulation function $f_i(t)$ in the neuron model summarized in Table 1. We extend these dynamics to build a coupled network with interesting properties like memory and global adaptation for energy-efficient neural representation. The results reported here are representative of the types of dynamical properties the proposed model can exhibit, but are by no means exhaustive. Readers are encouraged to experiment with different inputs and network parameters in the software (MATLAB) implementation of the Growth Transform neuron model [14]. The tool enables users to visualize the effects of different modulation functions and other hyperparameters on the neural dynamics, as well as the time-evolution of population trajectories and the network energy function with different inputs and under different initial conditions.

First, we present the results for an uncoupled network, with

$$Q_{ij} = \begin{cases} 1 & ; \quad \forall i = j \\ 0 & ; \quad \forall i \neq j \end{cases} . \tag{29}$$

The input-output characteristics for the spiking neuron model is plotted in Fig. 3(a). As v_i exceeds the threshold for a positive stimulus, the neuron enters a spiking regime and the firing rate changes almost linearly with the input, whereas the sub-threshold response is similar to the non-spiking case.

5.1 Standard uncoupled tonic-spiking response

When stimulated with a constant current stimulus b_i, a vast majority of neurons fire single, repetitive action potentials for the duration of the stimulus, with or without adaptation [23, 24, 25].

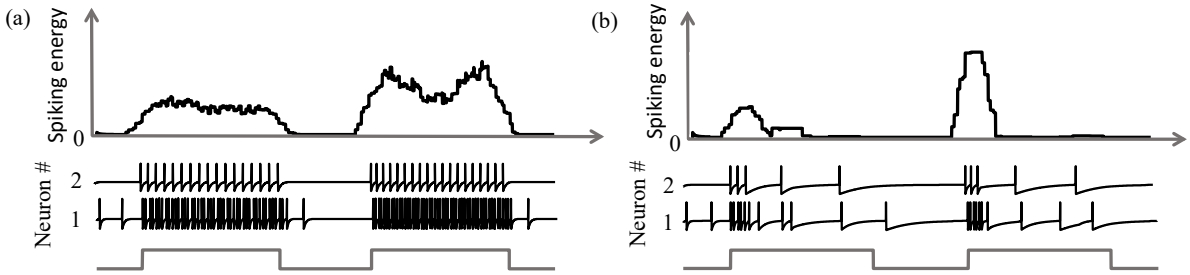

Figure 5: Mean spiking energy $\int \Psi(v_i)dv_i$ and firing patterns in response to a step input (a) without global adaptation; (b) with global adaptation.

The proposed model shows tonic spiking without adaptation when the modulation function $f_{i,n} = f$, where $0 < f \leq 1$. A simulation of tonic spiking response using the neuron model is given in Fig. 3(b).

5.2 Uncoupled tonic-spiking response with maximum hyperpolarization

The state of hyperpolarization reached by the neuron immediately after a spike can be tuned by varying the constant f, which regulates the speed of the growth transform updates at a particular point. The fastest rate at which the updates could take place corresponds to $f_{i,n} = 1$, leading to maximum hyperpolarization. The modulation function in this case is varied as follows

$$f_{i,n} = \begin{cases} f & ; \quad v_{i,n} < 0 \\ 1 & ; \quad v_{i,n} \geq 0 \end{cases} \quad , \quad f \in (0, 1]. \tag{30}$$

Simulation for uncoupled tonic-spiking response with maximum hyper-polarization is given in Fig. 3(c) for the same input as in (b). It can be seen that the neuron reaches a more hyperpolarized state after each spike in this case, which increases the time required to reach the threshold once more, thereby regulating the firing rate.

5.3 Uncoupled bursting response with maximum hyperpolarization

Bursting neurons fire discrete groups of spikes interspersed with periods of silence in response to a constant stimulus [23, 24, 26, 27]. Bursting arises from an interplay of fast ionic currents responsible for spiking, and slower intrinsic membrane currents that modulate the spiking activity, causing the neuron to alternate between activity and quiescence. Bursting response can be simulated in the proposed model by modulating $f_{i,n}$ at a slower rate compared to the generation of action potentials, in the following way

$$f_{i,n} = \begin{cases} f & ; \quad c_{i,n} < B \\ 1 & ; \quad c_{i,n} \geq B \end{cases} \tag{31}$$

where B is a hyper-parameter and the count variable $c_i(n)$ is updated according to

$$c_{i,n} = \begin{cases} c_{i,n-1} + \Psi(v_{i,n}) & ; \quad c_{i,n-1} < B \\ 0 & ; \quad c_{i,n-1} \geq B \end{cases} \tag{32}$$

Simulation of a bursting neuron in response to a step input is given in Fig. 3(d).

5.4 Uncoupled tonic-spiking response with adaptation

When presented with a prolonged stimulus of constant amplitude, many cortical cells initially respond with a high-frequency spiking that decays to a lower steady-state frequency [28]. This

adaptation in the firing rate is caused by a negative feedback to the cell excitability due to the gradual inactivation of depolarizing currents or activation of slow hyperpolarizing currents upon depolarization, and occur at a time-scale slower than the rate of action potential generation. We modeled spike-frequency adaptation by varying the modulation function according to

$$f_{i,n} = \begin{cases} \sigma[-h_n * \Psi(v_{i,n})] & ; \quad v_{i,n} < 0 \\ 1 & ; \quad v_{i,n} \geq 0, \end{cases} \tag{33}$$

where $h_n * \Psi(v_{i,n})$ is a convolution operation between the time-domain filter h_n and the spiking function $\Psi(v_{i,n})$, and

$$\sigma(x) = b\left[1 + \frac{1}{1 + \exp(-x)}\right] \tag{34}$$

is a sigmoidal function ensuring $1 > f_{i,n} > 0$. The parameter $b \in (0, 1)$ determines the steady-state firing rate for a particular stimulus. For the results, the smoothing filter h_n has been chosen to be

$$H(z) = \frac{1}{1 - 0.99z^{-1} - 0.01\log_2(1+\beta)z^{-1}}, \tag{35}$$

where $\beta > 0$ is a hyper-parameter for tuning the first-order filter response. As the neuron spikes, f decreases, slowing down the growth-transform neuron updates until the frequency reaches a lower constant value. A tonic-spiking response with adaptation is shown in Fig. 3(e).

5.5 Integrator response

When the baseline input is set slightly negative so that the fixed point is below the threshold, the neuron works like a leaky integrator as shown in Fig. 3(f), preferentially spiking to high-frequency or closely-spaced input pulses that are more likely to make v_i cross the threshold.

5.6 Ramp response

Commonly, the firing rate in neurons increases smoothly with the strength of the injected current, giving rise to a continuous frequency-current curve. A similar response of the proposed neuron model to a ramp input is plotted in Fig. 3(g).

5.7 Coupled spiking network with pre-synaptic adaptation

We can extend the proposed framework to a network model where the neurons, apart from external stimuli, receive inputs from other neurons in the network. We begin by considering $\mathbf{Q}$ to be a positive-definite matrix, which gives an unique solution of (16). Interactions among the neurons in a coupled network can be captured by the modulation function as follows

$$f_{i,n} = \begin{cases} \sigma[h_n * \sum_j Q_{ij}\Psi(v_{j,n})] & ; \quad v_{i,n} < 0 \\ 1 & ; \quad v_{i,n} \geq 0 \end{cases}, \tag{36}$$

with the compressive-function $\sigma(.)$ and the smoothing-filter $h(n)$ given by (34) and (35). This ensures that $Q_{ij} > 0$ corresponds to an excitatory coupling from the pre-synaptic neuron j, and $Q_{ij} < 0$ corresponds to an inhibitory coupling, as demonstrated in Fig. 4(a). Fig. 4(b) illustrates how different variations of the modulation function under the same energy landscape leads to the neurons following different response trajectories and converging to varying limit-cycles. The energy contours for a two-neuron network corresponding to a particular $\boldsymbol{Q}$ with excitatory and inhibitory connections and a fixed stimulus vector $\boldsymbol{b}$ are plotted, along with the responses of the two neurons starting from the same initial conditions, with and without pre-synaptic adaptation (where the latter corresponds to the case where neither neuron can integrate inputs from the other neuron). Because the energy landscape is the same in both cases, the neurons converge to the same sub-domain, but with widely varying trajectories and steady-state response patterns.

5.8 Coupled network with pre-synaptic and global adaptation

Apart from the pre-synaptic adaptation that changes individual firing rates based on the inputs received by each neuron, neurons in the coupled network can be made to adapt according to the global dynamics by changing the modulation function as follows

$$f_{i,n} = \begin{cases} \sigma[h_n * (\sum_j Q_{ij}\Psi(v_{j,n}) + \mathcal{F}(\mathcal{H}, \dot{\mathcal{H}})] & ; \quad v_{i,n} < 0 \\ 1 & ; \quad v_{i,n} \geq 0 \end{cases} \tag{37}$$

with the compressive-function $\sigma(.)$ and smoothing-filter h_n given by (34) and (35). The new function $\mathcal{F}(.)$ is used to capture the dynamics of the network cost-function. As the network starts to stabilize and converge to a fixed-point, the function $f_i(.)$ adapts to reduce the spiking rate of the neuron without affecting the steady-state solution. Fig.s 5(a) and (b) shows the time-evolution of the mean population firing rate r and the spike-trains for a two-neuron network without global adaptation and with global adaptation respectively, using a form for the adaptation term as given below

$$\mathcal{F}(\mathcal{H}, \dot{\mathcal{H}}) = \begin{cases} -\sigma[h_n * \mathcal{E}_t(\mathcal{H})] & ; \quad \mathcal{E}_t(\dot{\mathcal{H}}) \approx 0 \\ 0 & ; \quad \text{otherwise.} \end{cases} \tag{38}$$

This feature is important in designing energy-efficient spiking networks where energy is only dissipated during transients.

5.9 Coupled spiking network with non-positive definite Q

As illustrated in Fig. 6, a coupled spiking network can function as a memory element, when $\mathbf{Q}$ is a non-positive definite matrix and

$$f_{i,n} = \begin{cases} \sigma[h_n * \sum_j Q_{ij}\Psi(v_{j,n})] & ; \quad v_{i,n} < 0 \\ 1 & ; \quad v_{i,n} \geq 0 \end{cases} \tag{39}$$

due to the presence of more than one attractor state. We demonstrate this by considering two different orders of stimulus presentation in a network of four neurons, where a stimulus 'Stim 1' precedes another stimulus 'Stim 2' in Fig.s 6(a), (c) and (e), and a third stimulus 'Stim 3' precedes 'Stim 2' in Fig.s 6(b), (d) and (f). Here, each 'stimulus' essentially corresponds to a different input vector $\boldsymbol{b}$. For an uncoupled network, where neurons do not receive any inputs from other neurons, the network energy increases when the first stimulus is applied and returns to zero afterwards, and the network begins from the same state again for the second stimulus as for the first, leading to the same firing pattern for the second stimulus, as shown in Fig.s 6(a) and (b), independent of the history. For a coupled network with a positive definite synaptic weight matrix Q, reinforcing loops of spiking activity in the network may not allow the network energy to go to zero after the first stimulus is removed, and the residual energy may cause the network to exhibit a baseline activity that depends on stimulus history, as long as there is no dissipation. When the second stimulus is applied, the initial conditions for the network are different for the two stimulus histories, leading to two different transients until the network settles down into the same steady-state firing patterns, as shown in Fig.s 6(c) and (d). For a non-positive definite synaptic weight matrix Q however, depending on the initial condition, the network may settle down to different solutions for the same second stimulus, due to the possible presence of more than one local minimum. This leads to completely different transients as well as steady-state responses for the second stimulus, as shown in Fig. 6(e) and (f). This history-dependent stimulus response could serve as a short-term memory, where residual network energy from a previous external input subserves synaptic interactions among a population of neurons to set specific initial conditions for a future stimulus based on the stimulus history, forcing the network to settle down in a particular attractor state.

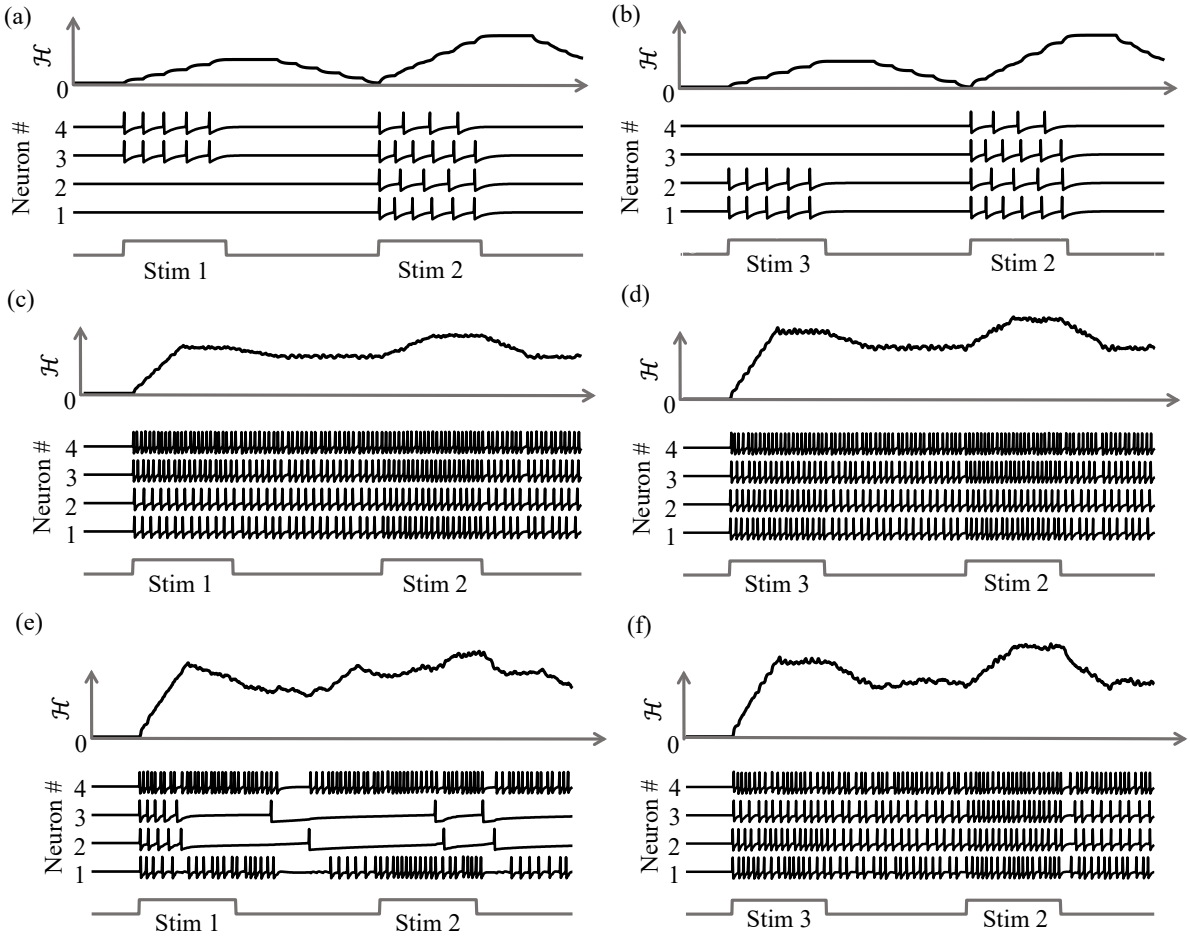

Figure 6: Stimulus response for a 4-neuron network with different stimulus histories for: (a)-(b) an uncoupled network; (c)-(d) a coupled network with a positive definite synaptic weight matrix; (e)-(f) a coupled network with a non-positive definite synaptic weight matrix.

6 Conclusions

This paper introduces the theory behind a new spiking neuron and population model based on the Growth transform dynamical system. The system minimizes an appropriate energy functional under realistic physical constraints to produce emergent spiking activity in a population of neurons. The neuron model and its response are tightly coupled to the network objective, and is flexible enough to incorporate different neural dynamics that have been observed at the cellular level in electrophysiological recordings. In each of these experiments, the spiking activity is modulated externally by allowing a slower modulation function to evolve in different ways, without affecting the underlying optimization process. This allows the network to reach the same asymptotic fixed-point through many possible response trajectories, and using widely varying encoding techniques. The model can be easily extended to a coupled network of neurons, which can be tweaked to exhibit useful properties like memory and global adaptation for energy-efficiency.

The paper is accompanied by a software tool [14] that enables readers to visualize the effects of different model parameters on the neural dynamics. Many more neural dynamics can be simulated using the model and readers are encouraged to experiment with different network hyper-parameters. The paper and the tool illustrate how spike generation and spike-based encoding in an artificial neuron model can be framed as a network-level energy optimization problem, thereby providing a framework to develop scalable and energy-efficient neuromorphic machine learning algorithms. Currently, the model only considers fixed synaptic weights Q_{ij}. Future research will investigate learning and adapting these weights for an optimal neural representation, or for solving a particular task.

References

[1] G. N. Borisyuk, R. M. Borisyuk, A. I. Khibnik, and D. Roose, "Dynamics and bifurcations of two coupled neural oscillators with different connection types," *Bulletin of mathematical biology*, vol. 57, no. 6, pp. 809–840, 1995.

[2] W. Maass, T. Natschläger, and H. Markram, "Real-time computing without stable states: A new framework for neural computation based on perturbations," *Neural computation*, vol. 14, no. 11, pp. 2531–2560, 2002.

[3] J. J. Hopfield and D. W. Tank, "neural computation of decisions in optimization problems," *Biological cybernetics*, vol. 52, no. 3, pp. 141–152, 1985.

[4] D. J. Amit, H. Gutfreund, and H. Sompolinsky, "Spin-glass models of neural networks," *Physical Review A*, vol. 32, no. 2, p. 1007, 1985.

[5] ——, "Storing infinite numbers of patterns in a spin-glass model of neural networks," *Physical Review Letters*, vol. 55, no. 14, p. 1530, 1985.

[6] E. Agliari, A. Barra, A. Galluzzi, D. Tantari, and F. Tavani, "A walk in the statistical mechanical formulation of neural networks," *arXiv preprint arXiv:1407.5300*, 2014.

[7] D. Horn and M. Usher, "Neural networks with dynamical thresholds," *Physical Review A*, vol. 40, no. 2, p. 1036, 1989.

[8] Z. Jonke, S. Habenschuss, and W. Maass, "Solving constraint satisfaction problems with networks of spiking neurons," *Frontiers in neuroscience*, vol. 10, p. 118, 2016.

[9] T. Nakano, M. Otsuka, J. Yoshimoto, and K. Doya, "A spiking neural network model of model-free reinforcement learning with high-dimensional sensory input and perceptual ambiguity," *PloS one*, vol. 10, no. 3, p. e0115620, 2015.

[10] J. Burroni, P. Taylor, C. Corey, T. Vachnadze, and H. T. Siegelmann, "Energetic constraints produce self-sustained oscillatory dynamics in neuronal networks," *Frontiers in neuroscience*, vol. 11, p. 80, 2017.

[11] Y. LeCun, S. Chopra, R. Hadsell, M. Ranzato, and F. Huang, "A tutorial on energy-based learning," *Predicting structured data*, vol. 1, no. 0, 2006.

[12] A. Gangopadhyay and S. Chakrabartty, "Spiking, bursting, and population dynamics in a network of growth transform neurons," *IEEE transactions on neural networks and learning systems*, vol. 29, no. 6, pp. 2379–2391, 2018.

[13] E. M. Izhikevich, "Which model to use for cortical spiking neurons?" *IEEE transactions on neural networks*, vol. 15, no. 5, pp. 1063–1070, 2004.

[14] D. Mehta, A. Gangopadhyay, K. Aono, and S. Chakrabartty, "Growth transform neuron model matlab gui," https://github.com/aimlab-wustl/growth-transform-NN, 2019.

[15] P. Gopalakrishnan, D. Kanevsky, A. Nadas, and D. Nahamoo, "A generalization of the baum algorithm to rational objective functions," in *Acoustics, Speech, and Signal Processing, 1989. ICASSP-89., 1989 International Conference on.* IEEE, 1989, pp. 631–634.

[16] O. Chatterjee and S. Chakrabartty, "Decentralized global optimization based on a growth transform dynamical system model," *IEEE Transactions on Neural Networks and Learning Systems*, 2018.

[17] L. E. Baum and G. Sell, "Growth transformations for functions on manifolds," *Pacific Journal of Mathematics*, vol. 27, no. 2, pp. 211–227, 1968.

[18] C. Koch and T. Poggio, "Biophysics of computation: neurons, synapses and membranes," 1984.

[19] A. L. Hodgkin and A. F. Huxley, "A quantitative description of membrane current and its application to conduction and excitation in nerve," *The Journal of physiology*, vol. 117, no. 4, pp. 500–544, 1952.

[20] R. FitzHugh, "Impulses and physiological states in theoretical models of nerve membrane," *Biophysical journal*, vol. 1, no. 6, pp. 445–466, 1961.

[21] E. M. Izhikevich, "Simple model of spiking neurons," *IEEE Transactions on neural networks*, vol. 14, no. 6, pp. 1569–1572, 2003.

[22] A. Gore and S. Chakrabartty, "A min-max optimization framework for designing σ learners: Theory and hardware," *IEEE Trans. Circuits Syst. I*, vol. 57, no. 3, pp. 604–617, 2010.

[23] A. Agmon and B. Connors, "Repetitive burst-firing neurons in the deep layers of mouse somatosensory cortex," *Neuroscience letters*, vol. 99, no. 1-2, pp. 137–141, 1989.

[24] D. A. McCormick, B. W. Connors, J. W. Lighthall, and D. A. Prince, "Comparative electrophysiology of pyramidal and sparsely spiny stellate neurons of the neocortex," *Journal of neurophysiology*, vol. 54, no. 4, pp. 782–806, 1985.

[25] J. R. Gibson, M. Beierlein, and B. W. Connors, "Two networks of electrically coupled inhibitory neurons in neocortex," *Nature*, vol. 402, no. 6757, p. 75, 1999.

[26] C. M. Gray and D. A. McCormick, "Chattering cells: superficial pyramidal neurons contributing to the generation of synchronous oscillations in the visual cortex," *Science*, vol. 274, no. 5284, pp. 109–113, 1996.

[27] J. C. Brumberg, L. G. Nowak, and D. A. McCormick, "Ionic mechanisms underlying repetitive high-frequency burst firing in supragranular cortical neurons," *Journal of Neuroscience*, vol. 20, no. 13, pp. 4829–4843, 2000.

[28] B. W. Connors and M. J. Gutnick, "Intrinsic firing patterns of diverse neocortical neurons," *Trends in neurosciences*, vol. 13, no. 3, pp. 99–104, 1990.